

## Preliminary Palaeomagnetic Characterisation of Basalts from Northeast Lebanon

Abdul Sahib Abdul Lateef

Previously of the Geology and Mineralogy Department, Royal Museum for Central Africa-Tervuren-Belgium.

\* Corresponding Author: [abdulsah@yahoo.com](mailto:abdulsah@yahoo.com)

Received: 21 July 2016 / Accepted: 06 October 2016 / Published online: 10 October 2016

---

### Abstract

A preliminary palaeomagnetic results from basalt outcrops in northeast Lebanon is reported. The remanence carrier of the characteristic magnetisation is magnetite. Both variations of susceptibility and anisotropy directional data show that the measured directions of thermoremanent magnetisation (TRM) are representative of the ambient field at the time of cooling of these basalts through their blocking temperature. The natural remanent magnetism (NRM) and thermal and alternating field (AF) demagnetisation experiments indicate two magnetic components: 1) Normal polarity component and 2) Transitional/intermediate polarity component that imply two basaltic emplacements. The normal component is correlated to the long normal polarity subchron C5n.2n while the transitional / intermediate component is possibly related to a cryptochron within C5n.2n.

**Keywords:** Palaeomagnetism; Basalt; Bekaa Valley; Lebanon.

### 1- Introduction

Previous palaeomagnetic studies in Lebanon (e.g. Van Dongen *et al.*, 1967; Gregor *et al.*, 1974; Henry *et al.*, 2010) have been carried out on Mesozoic and Cenozoic rocks to solve structural and tectonical problems. In comparison, the present investigation is limited in scope and aim to constrain further a newly reported Miocene volcanics (Lateef, 2014) by providing their partial palaeomagnetic characteristics and acquire initial polarity decision. The location of the studied basalts is given in Figure 1. Photographs illustrating some features of the sampled localities are shown on Figs. 2 and 3.

### 2- Materials and methods

Palaeomagnetic analysis is directional; hence oriented samples are needed. In the present reconnaissance study, oriented block samples have been collected as illustrated in Figure 4.

A total of 17 oriented samples have been collected from the two basalt localities (Table 1). Nine samples from Al-Qamoua location; four from site-1 (Qam 11, Qam 12, Qam 13, Qam 14), three from site-2 (Qam 25, Qam 26, Qam 27) and two from site 3 (Qam 38, Qam 39). From the second, northern Jisr Al-Asi location that represents one site, eight samples have been collected (Asi 11, Asi 12, Asi 13, Asi 14, Asi 15, Asi 16, Asi 17, Asi 18). Sample code designation constitutes first of three letters denoting the abbreviation of the location name, this is followed by two figures: the first is for site number while the second stands for the sample number.

All laboratory work has been carried out in the palaeomagnetism facility of the Centre of Physics of Earth, Dourbes, Belgium.

In the laboratory, the collected samples have been restored to their field position by making use of the field measurements. The samples were vertically drilled and multiple cores

obtained from each sample (Except sample Asi 11, which has been lost during transport). Vertical coring assures that the AB direction will be tangent to the vertical fiducial mark on each cylindrical specimen (hence no need to transfer the AB direction for each cylindrical specimen). Later, slices or multiple specimens were prepared from each cylindrical core. A total of 34 specimens were obtained from the 9 samples from Al Qamoua location, and 24 specimens were obtained from the 7 samples from Jisr Al Asi location. Each slice is labelled with a mark indicating the top of the specimen. Specimens represent the highest level in the hierarchy of palaeomagnetic sampling scheme, and this is denoted by a third number (Specimen number) in the sample code (Table 2).

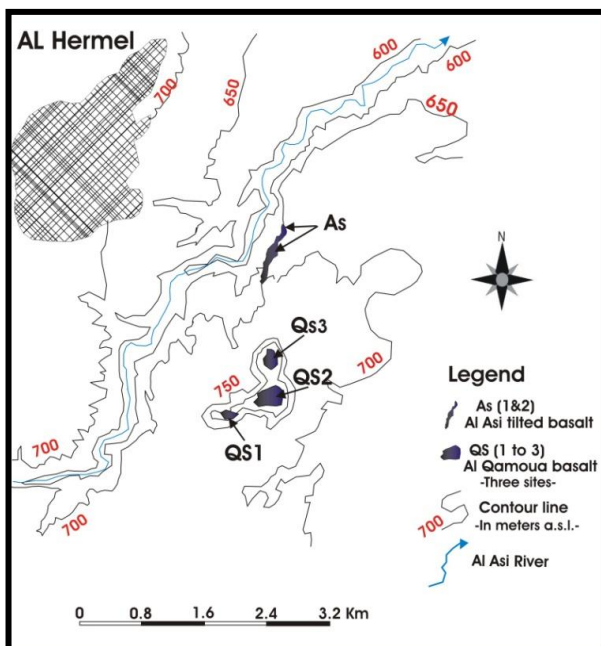


Figure 1) Location and associated topography of the sampled basalt outcrops. There are two sampled locations situated between Al Asi River Bridge and the archaeological column (Obelisk) of Al Qamoua. The northern Jisr Al Asi basalt localition (As), nearby Al Asi Bridge, is considered one sampling site representing single flow. It is a concordant, tilted basalt body within the clastic sequence of Al-Hermel Formation. The southern basalt localition (Qs) has a hillocky topography and comprises three sampling points (Qs1, Qs2 and Qs3) where each site is associated with distinctive physiographic dome formed by a basalt plug.



Figure 2) View from site Qs3 (Tell Abu Tineh). The view, a small quarrying pit, doesn't show the sampled basalt body but the criss-cross basalt veins (Micro sill and dike) within a metamorphosed (baked) host rock. Ballpoint pen stands for a scale.

### 3- Results

A Triaxial cryogenic magnetometer (2G Enterprises) was used for remanence measurements. For magnetic cleaning experiments a triple Mu metal- shielded Schonstedt GSD-1 Alternating Field demagnetiser and Schonstedt TSD-1 Thermal Demagnetiser were used. KappaBridge KLY-3 and software SUSAR version 1.4 have been utilized in magnetic susceptibility measurements (k).

#### 3.1- Natural Remanent Magnetisation (NRM)

Initially, the NRMs of all samples were measured. The most important measured parameters are shown in Table 3 and Table 4. The related equal area stereographic projections of non-cleaned NRM directions are provided by Figs. 5, 6 and 7.

#### 3.2- Demagnetisation

To remove soft, low-stability components of the NRM and isolate the high-stability components or the characteristic NRM (ChNRM), both thermal and alternating field (AF) demagnetisation has been applied on pilot samples. Both cleaning techniques tend to randomize unstable magnetic components of

secondary origin that have lower coercive force (alternating field demagnetisation) or with low Curie temperatures (thermal demagnetisation). A total of seven specimens, three from the

northern Al Asi location and four from the southern Al Qamoua location, have been selected for the demagnetisation experiments.



Figure 3) Al Asi basalt, the northern sampling location (As). (a) Basalt outcrop exposed by a road-cut, which exhibits spheroidal weathering forms guided by joints that are seen marked by whitish carbonate alteration product. (b) The tilted basalt ( $29^\circ$  due west) of the basalt horizon is shown (Head of the downward arrow). In the background is monoclonal flexure with calcrete carapace that covers the underlying sequence of Al Hermel Formation (Mudstone with interbedded conglomerate). In the far northwestern corner of the view is Al Hermil town. View looks northwestwards.

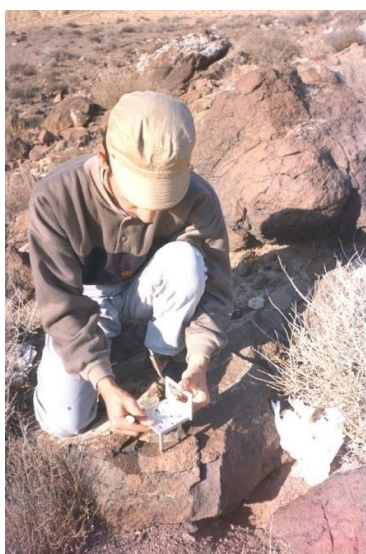


Figure 4) Procedure for oriented block sampling (Qs1 sampling site). Leveled tripod with sideways clinometers is used. The three legs of the tripod are labeled A, B and C respectively. First, the tripod was set with its two points A and B forming horizontal line with B pointed toward north. After marking the position of both points on the outcrop, the azimuth (with respect to north) of the AB line is measured using magnetic compass (no observable effect was found on the magnetic needle of the compass as one moves away or towards the

outcrop). After, the tripod is inclined until the third leg C meets the surface of the outcrop. The clinometer reading then registers the inclination (maximum angle of slope of the upper surface of sample, in degrees). After the A, B and C positions are marked on the outcrop, the sample is carefully removed from the outcrop. In the case of the northern sampling locality (As) the dip amount and direction of the tilted basalt are recorded.

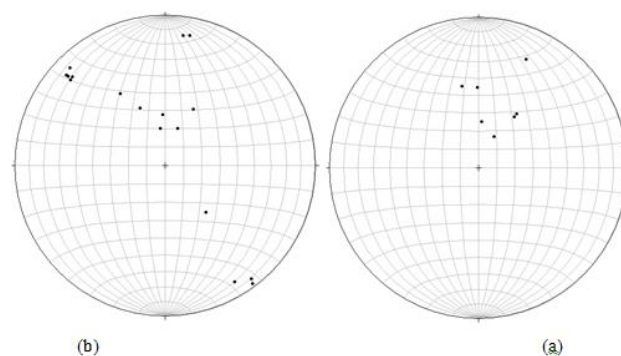


Figure 5) Equal area stereographic projection of the NRM directions (a) Al Qamoua site-1 and (b) Al Qamoua site 2. Both plots show northward and down (positive) inclinations that provisionally define a Normal polarity. Site-2 displays lower scatter/lower incoherence in comparison to site-1.

### 3.3- Thermal Demagnetisation

Progressive stepwise thermal demagnetisation was carried on five pilot samples; two from Al Asi location (samples Asi 131 and Asi 184) and three from Al Qamoua location (samples Qam 125, Qam 271 and Qam 381). Starting from room temperature of 25°C, thermal cleaning was carried along successive heating thresholds of 100°C, 140°C, 180°C, 220°C, 260°C, 300°C, 340°C, 380°C, 420°C, 460°C, 500°C, 530°C, 560°C and finally 590°C. The changes of remanence intensity during thermal demagnetisation are shown in Table 5 and Figure 8. The graphical plot of the observed change in NRM is shown on Figure 8.

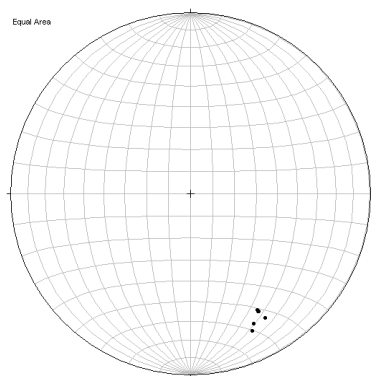


Figure 6) Equal area stereographic projection of the NRM directions Al Qamoua site-3. The data

show well clustering with southward declination and (down) positive inclination that provisionally indicates transitional/intermediate polarity, which is clearly in contrast with the other two Al Qamoua sites (Qam 1 and Qam 2). This assumes significance when compared to the deduced polarity from the other Jisr Al Asi location (see next section).

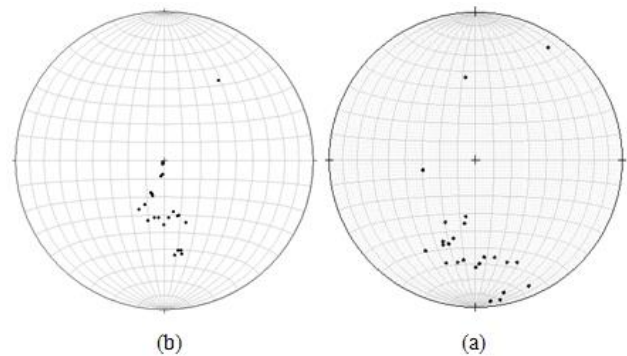


Figure 7) Equal area stereographic projection of the NRM directions, Al Asi site (Jisr Al Asi location) before (a) and after (b) tilt correction. The distribution of NRM after tilt correction shows more scatter (lower clustering), which can be attributed to secondary NRM component acquired after tilting. The plot indicates transitional/intermediate polarity with southward declination and down (positive) inclination which make this site comparable to NRM directions of Qam 3 site.

Table 1) The collected oriented block samples and associated field measurements from Al-Qamoua and Jisr el Asi locations.

Location	Site	Sample No.	AB-Azimuth	Clinometer	Remarks
Al-Qamoua	1	1	N40°W	49°	Unnamed
Al-Qamoua	1	2	N70°W	53°	Unnamed
Al-Qamoua	1	3	N100°E	41°	Unnamed
Al-Qamoua	1	4	N14°E	52°	Unnamed
Al-Qamoua	2	5	N25°W	30°	Al-Qamoua monument
Al-Qamoua	2	6	N75°E	44°	Al-Qamoua monument
Al-Qamoua	2	7	N60°E	47°	Al-Qamoua monument
Al-Qamoua	3	8	N	21.5°	Tell Abu Tineh
Al-Qamoua	3	9	N18°E	27°	Tell Abu Tineh
Jisr Al-Asi	1	1	N20°E	40°	from base of bed
Jisr Al-Asi	1	2	N10°W	50°	
Jisr Al-Asi	1	3	N25°E	28°	
Jisr Al-Asi	1	4	N10°W	24°	exceptionally "A" is toward north
Jisr Al-Asi	1	5	N5°E	30°	
Jisr Al-Asi	1	6	N20°E	38°	
Jisr Al-Asi	1	7	N	32°	southern extension of outcrop
Jisr Al-Asi	1	8	N8E	40°	southern extension of outcrop

N.B. in the AB azimuth "B" is toward north except for sample 4 of Jisr Al-Asi locality.

Table 2) Specimens prepared from the oriented block samples.

Sample no._	Specimens no.
Qam 11	Qam 111, Qam 112, Qam 113, Qam 114, Qam 115
Qam 12	Qam 121, Qam 122, Qam 123, Qam 124, Qam 125, Qam 126
Qam 13	Qam 131, Qam 132, Qam 133, Qam 134,
Qam 14	Qam 141, Qam 142, Qam 143, Qam 144
Qam 25	Qam 251, Qam 252, Qam 253
Qam 26	Qam 261, Qam 262, Qam 263
Qam 27	Qam 271, Qam 272
Qam 38	Qam 381, Qam 382, Qam 383
Qam 39	Qam 391, Qam 392, Qam 393, Qam 394
Asi 11	Missing
Asi 12	Asi 121, Asi 122
Asi 13	Asi 131, Asi 132, Asi 133
Asi 14	Asi 141, Asi 142
Asi 15	Asi 151, Asi 152, Asi 153
Asi 16	Asi 161, Asi 162, Asi 163
Asi 17	Asi 171, Asi 172, Asi 1, Asi 174
Asi 18	Asi 181, Asi 182, Asi 183, Asi 184, Asi 185, Asi 186

Curves of the five specimens don't display similar behaviour because of difference in stability and presence of different magnetic phases or components (magnetic mineral assemblage) and hence different Curie points. As for the spectrum of stability it can be observed that in variance with others, specimen Qam 271 reflects rapid decrease of NRM below 300°C with 10%-20% of the original remanence remained at this temperature. This specimen has curie points at 300-320°C that could not be identified well, at 420°C that could be associated with titanomagnetite or tetranomagemite (Ti-iron oxides) and at 500-590°C related to magnetite. As for specimen asi 131, a phase can be seen in the range 260°C - 280°C, another is that of Magnetite with the highest Curie point. For specimen Asi 284 three phases may be recognized, one at the range 300-320°C, another at 500°C that could lead to a spectrum towards 590°C. For specimen Qam 125, a Curie point can be identified at 420°C and then the range for the Magnetite curie spectrum between 500 and 590. In specimen

Qam 381 there is a phase at 420°C and another at the maximum of magnetite, 590 °C. These magnetic phases are the cause for the drop of magnetic intensity around the corresponding temperatures as seen in the above figure. Note that the absence of low blocking temperatures (soft magnetism) and high average median destructive fields both indicate high stability of remanence. For all specimens, the blocking temperature of the characteristic component ranges from 440 to 590° C. Such variability is suggestive of variable mineralogic concentration.

### 3.4- Alternating Field (Af) Demagnetisation

Two pilot specimens, one from Al Asi locality (Asi 185) and the other from Al Qamoua locality specimen Qam 382 have been selected for alternating field (AF) demagnetisation experiments. The specimens were treated in successive alternating fields of 25 (d.r.2.5), 50 (d.r.2.5), 75(d.r.5), 100(d.r.5), 150(d.r.10), 200(d.r.10), 250(d.r.10), 300(d.r.25), 400(d.r.25), 500(d.r.25), 600(d.r.50), 800(d.r.50) and 600(d.r.50) Oersted [d.r. stands

for the corresponding "decay rate" at each A.F. peak value]. The record of NRM at successive AF demagnetisation steps for the two samples is shown in Table 6 and the plot of the observed change in magnetisation is shown on Figure 9.

Table 3) Pre-demagnetisation-natural remanent magnetisation (NRM), all specimens, southern Al Qamoua.

Specimen	Az+X	Weight(g)	D	I	J	Remarks
Qam 111	54°	33.05				
112	54°	32.95	18.4	68.6	5.097 e-3	
113	54°	33.38	352.9	69.6	5.437 e-3	
114	54°	33.18	336.4	55.6	4.038 e-3	
115	54°	31.96	328	42.7	3.151 e-3	
Qam 121	24°	32.78	312.5	11.7	2.154 e-3	
122	24°	32.98	357	62.1	2.521 e-3	
123	24°	31.78	312.5	13	2.042 e-3	
124	24°	32.56	315.8	9.7	1.930 e-3	
125	24°	32.53	313.8	15.4	2.165 e-3	Pilot specimen for thermal DM.
126	24°	32.25	312.1	16	2.040 e-3	
Qam 131	194°	32.99	142.7	5.3	3.131 e-3	
132	194°	32.38	139.2	55.9	4.309 e-3	
133	194°	32.65	143.4	2	3.426 e-3	
134	194°	31.74	149.1	10.6	2.612 e-3	
Qam 141	108°	32.58	10.8	12.7	2.132 e-3	
142	108°	32.62	7.9	13.4	2.346 e-3	
143	108°	32.25	26.8	55.4	3.061 e-3	
144	108°	32.18				Discarded specimen
Qam 251	69°	32.9	348.2	43.8	1.258 e-3	
252	69°	32.98	3.9	64.8	3.756 e-3	
253	69°	31.89	359.2	45.4	1.102 e-3	
Qam 261	169°	33.09	23.8	21.8	1.246 e-3	
262	169°	32.91	26.9	71.1	3.001 e-3	
263	169°	32.89				Discarded specimen
Qam 271	154°	33.31	35.3	55.8	1.023 e-3	Pilot specimen for thermal DM.
272	154°	33.41	35.3	53.5	9.837 e-4	
Qam 381	94°	31.59	150	25.6	2.495 e-3	Pilot specimen for thermal DM.
382	94°	31.33	149.9	26.5	2.096 e-3	Pilot specimen for A.F.DM.
383	94°	31.58	149.9	25.5	2.523 e-3	
Qam 391	112°	31.41	148.7	20.8	1.736 e-3	
Qam 392	112°	31.07	154	21	2.132 e-3	
Qam 393	112°	31.83				Discarded specimen
Qam 394	112°	28.89	155.5	17.7	1.679 e-3	

Table 4) Pre-demagnetisation: natural remanent magnetisation (NRM), all specimens, northern Jisr Al Asi.

Specimen	Az+X	Weight (gm)	D	I	J	Remarks
Asi 121	84°	32.99	202.7	71	4.949 e-4	
Asi 122		32.96	198.6	69.6	5.950 e-4	
Asi 131	119°	33.15	227.1	88.7	2.035 e-3	Pilot sample for thermal D.M.
Asi 132		33.07	200.2	70.5	3.353 e-4	
Asi 133		32.53	204.1	63.5	4.911 e-4	
Asi 141	264°	32.69	195.6	55.5	1.245 e-3	
Asi 142		29.27	207.5	59.6	1.062 e-3	
Asi 151	99°	32.82	186	58.3	1.201 e-3	
Asi 152		32.95	33.9	35.1	1.822 e-3	
Asi 153		32.95	190.2	57.8	1.105 e-3	
Asi 161	114°	33.92	193.4	81.4	3.811 e-3	
Asi 162		33.34	187.9	82.6	4.968 e-3	
Asi 163		33.9	175.9	58.4	9.947 e-4	
Asi 171	94°	32.77	169.9	61.5	8.005 e-4	
Asi 272		32.91	165.7	58.7	9.070 e-4	
Asi 273		32.89	205.4	87.9	5.756 e-4	
Asi 274		32.39	161	53.8	8.823 e-4	
Asi 181	102°	32.23	173.9	36.1	6.990 e-4	
Asi 182		31.96	166.7	58.7	1.224 e-3	
Asi 183		31.77	180.4	54.5	5.080 e-4	
Asi 184		31.66	169.7	36.4	7.088 e-4	Pilot sample for thermal D.M.
Asi 185		32.11	169.7	38.4	7.152 e-4	Pilot sample for A.F.Dem.
Asi 186		32.09	171.4	38.9	7.512 e-4	

Table 5) NRM record of five pilot samples (Asi 131, asi 184, Qam 125, Qam 271 and Qam 381) during thermal demagnetisation at successive heating steps.

Asi 131					Asi 184				
T (°C)	D	I	J(Am <sup>2</sup> Kg) e <sup>-3</sup>	J/J0	D	I	J(Am <sup>2</sup> Kg) e <sup>-4</sup>	J/J0	
20	358.1	87.8	2.044	1	189.2	35.5	6.794	1	
100	235.3	87	1.896	0.927592955	187.7	35.5	6.678	0.982926111	
140	219.8	88.7	1.724	0.843444227	193.5	34.1	6.533	0.96158375	
180	222	88	1.564	0.765166341	190.8	35.8	6.446	0.948778334	
220	217.2	87.7	1.414	0.691780822	187.7	34.5	6.398	0.941713276	
260	209.2	86.8	1.323	0.647260274	188.3	34.3	6.357	0.93567854	
300	214.1	82	1.38	0.675146771	188.7	34.4	6.221	0.915660877	
340	215.9	81.2	0.9927	0.485665362	186.3	34.7	5.799	0.853547248	
380	223	81.9	0.5271	0.257876712	188.5	37.1	4.457	0.656020018	
420	220.2	81.8	0.3373	0.165019569	191.5	39.4	3.565	0.524727701	
460	266.6	81.6	0.1386	0.067808219	190.5	43.4	2.416	0.355607889	
500	236.9	55.1	0.07768	0.038003914	190	43.7	1.983	0.291875184	
530	254.3	76.6	0.09598	0.046956947	189.4	43	1.796	0.264350898	
560	249.6	79.1	0.07924	0.038767123	192.6	46.8	1.213	0.178539888	
590	294.1	41.5	0.007987	0.003907534	258	68.2	0.0755	0.011112747	
Qam 125					Qam 271				
T (°C)	D	I	J (Am <sup>2</sup> /Kg) e <sup>-3</sup>	J/J0	D	I	J (Am <sup>2</sup> /Kg) e <sup>-4</sup>	J/J0	
20	47.3	14.5	2.118	1	6.7	55.1	10.04	1	
100	47	12.8	1.996	0.942398489	5.8	55.3	8.88	0.884462151	
140	48.6	12.6	1.691	0.798394712	6.5	58.7	7.492	0.746215139	
180	45.1	12.4	1.456	0.687440982	9	61.7	6.302	0.627689243	
220	45.2	13.2	1.261	0.595372993	11.1	63	4.672	0.465338645	
260	41.1	12.8	1.123	0.530217186	8.3	62.1	3.304	0.329083665	
300	37.4	12.9	0.928	0.438149197	358.2	59.8	1.471	0.146513944	
340	37.1	15.4	0.8221	0.388149197	358.3	59.3	1.759	0.175199203	
380	37.1	15.2	0.7106	0.335505194	8.4	60.1	2.26	0.225099602	
420	34.2	17	0.5839	0.275684608	1	61.5	2.248	0.223904382	
460	17.5	21.2	0.2915	0.137629839	2.8	63.9	1.028	0.102390438	
500	1.1	23.7	0.1901	0.089754485	4	72.8	0.4958	0.04938247	
530	342.3	25.1	0.1456	0.068744098	351.4	70.2	0.4053	0.040368526	
560	326.3	25.1	0.1099	0.051888574	349.6	71.3	0.2292	0.022828685	
590	309.8	23.4	0.01152	0.005439093	298.2	17.2	0.03113	0.003100598	
Qam 381									
T (°C)	D	I	J (Am <sup>2</sup> /Kg) e <sup>-3</sup>	J/J0					
20	175.4	26.1	2.368	1					
100	174.7	25.3	2.329	0.983530405					
140	175.8	24.8	2.218	0.936655405					
180	177.1	25.3	2.113	0.892314189					
220	176.7	25.1	1.997	0.843327703					
260	173.8	25.4	1.917	0.809543919					
300	173	26.1	1.798	0.759290541					
340	176.4	25.8	1.712	0.722972973					
380	174	26	1.605	0.677787162					
420	177.9	26.2	1.496	0.631756757					
460	181.5	25.5	1.16	0.489864865					
500	180.5	26.4	0.7476	0.315709459					
530	179.4	26.1	0.4255	0.1796875					
560	182.1	27.1	0.1677	0.070819257					
590	188	31	0.01653	0.006980574					

From the above thermal and AF coercivity of remanence is 1000-2000 Oe, demagnetisation experiments it appears that the which indicate magnetite as the carrier of the maximum blocking temperature is 590° C and characteristic magnetisation.

Table 6) Record of change in intensity of remanence for 2 pilot samples during AF demagnetisation.

QAM 382					ASI 185						
A.F	D	I	J	e <sup>-3</sup> (unified)	J/J0 Qam382	A.F	D	I	J	e <sup>-4</sup>	J/J0 Asi285
0	150	25.7	2.069 e <sup>-3</sup>	2.069	1	NRM	190.7	61.5	1.062 e <sup>-3</sup>	10.6	1
25	153	25.8	1.995 e <sup>-3</sup>	1.995	0.9642339	25	193.3	59.7	1.042 e <sup>-3</sup>	10.4	0.9811676
50	151	26.8	1.686 e <sup>-3</sup>	1.686	0.8148864	50	191.9	58.4	9.965 e <sup>-4</sup>	9.97	0.9383239
75	152	28.8	1.356 e <sup>-3</sup>	1.356	0.6553891	75	191.2	56.8	9.356 e <sup>-4</sup>	9.36	0.8809793
100	157	29.6	1.208 e <sup>-3</sup>	1.208	0.5838569	100	188	54.5	8.777 e <sup>-4</sup>	8.78	0.8264595
150	156	28.8	1.099 e <sup>-3</sup>	1.099	0.5311745	150	183.7	50.8	7.909 e <sup>-4</sup>	7.91	0.7447269
200	157	28.9	1.022 e <sup>-3</sup>	1.022	0.4939584	200	181.2	48.4	7.275 e <sup>-4</sup>	7.28	0.6850282
250	158	29	9.529 e <sup>-4</sup>	0.9529	0.4605607	250	178.7	45.8	6.738 e <sup>-4</sup>	6.74	0.6344633
300	157	27.9	8.915 e <sup>-4</sup>	0.8915	0.4308845	300	177.3	44.4	6.206 e <sup>-4</sup>	6.21	0.5843691
400	158	29.7	7.480 e <sup>-4</sup>	0.748	0.3615273	400	173.2	42.6	4.980 e <sup>-4</sup>	4.98	0.4689266
500	158	31	6.332 e <sup>-4</sup>	0.6332	0.3060416	500	170.5	43.2	3.711 e <sup>-4</sup>	3.71	0.349435
600	158	28.3	4.904 e <sup>-4</sup>	0.4904	0.2370227	600	172	44.1	2.728 e <sup>-4</sup>	2.73	0.2568738
800	158	29	3.145 e <sup>-4</sup>	0.3145	0.1520058	800	171.2	47.3	1.512 e <sup>-4</sup>	1.51	0.1423729
1000	154	29.6	2.013 e <sup>-4</sup>	0.2013	0.0972934	1000	171.6	50.9	9.130 e <sup>-5</sup>	0.91	0.0859699

Table 7) Values of remanence and calculated x, y, z values used for the z-plots for five thermally demagnetised pilot Samples.

Asi131									
T (°C)	D	I	J(Am <sup>2</sup> /Kg) e <sup>-3</sup>	J/J0	Drad	Irad	X	Y	Z
20	358.1	87.8	2.044	1	6.250024051	1.532399083	0.0784215	-0.002601511	2.042493401
100	235.3	87	1.896	0.927592955	4.10675973	1.518436449	-0.056489022	-0.081580509	1.893401598
140	219.8	88.7	1.724	0.843444227	3.836233696	1.548107047	-0.030049845	-0.025036587	1.723556258
180	222	88	1.564	0.765166341	3.874630939	1.535889742	-0.040562935	-0.036523031	1.563047253
220	217.2	87.7	1.414	0.691780822	3.790855135	1.530653754	-0.045200169	-0.034308796	1.412860875
260	209.2	86.8	1.323	0.647260274	3.651228795	1.514945791	-0.064466911	-0.036029339	1.320937131
300	214.1	82	1.38	0.675146771	3.736749929	1.431169987	-0.15903634	-0.107675697	1.366569935
340	215.9	81.2	0.9927	0.485665362	3.768165855	1.417207353	-0.123020246	-0.089051807	0.981014314
380	223	81.9	0.5271	0.257876712	3.892084232	1.429424657	-0.054316937	-0.050651363	0.52184147
420	220.2	81.8	0.3373	0.165019569	3.843215013	1.427679328	-0.036745264	-0.031052156	0.333851523
460	266.6	81.6	0.1386	0.067808219	4.653047786	1.42418867	-0.001200783	-0.020211469	0.137113145
500	236.9	55.1	0.07768	0.038003914	4.134684998	0.961676418	-0.024271115	-0.037231815	0.063709398
530	254.3	76.6	0.09598	0.046956947	4.438372288	1.336922207	-0.00601901	-0.02141331	0.093367029
560	249.6	79.1	0.07924	0.038767123	4.356341813	1.380555438	-0.005222977	-0.014044161	0.077810408
590	294.1	41.5	0.007987	0.003907534	5.13301333	0.72431164	0.002442596	-0.005460491	0.005292346
Asi284									
T (°C)	D	I	J(Am <sup>2</sup> /Kg) e <sup>-4</sup>	J/J0	Drad	Irad	X	Y	Z
20	189.2	35.5	6.794	1	3.302162945	0.619591884	-5.459950217	-0.88431897	3.945295881
100	187.7	35.5	6.678	0.982926111	3.275983006	0.619591884	-5.387642123	-0.728437795	3.877934338
140	193.5	34.1	6.533	0.96158375	3.377212103	0.595157275	-5.260247223	-1.262873626	3.662654551
180	190.8	35.8	6.446	0.948778334	3.330088213	0.624827872	-5.135513045	-0.979651507	3.770637173
220	187.7	34.5	6.398	0.941713276	3.275983006	0.602138592	-5.225215937	-0.706476913	3.623867104
260	188.3	34.3	6.357	0.93567854	3.286454982	0.598647933	-5.196501468	-0.75808758	3.582335093
300	188.7	34.4	6.221	0.915660877	3.293436299	0.600393263	-5.073969836	-0.77642649	3.514659728
340	186.3	34.7	5.799	0.853547248	3.251548396	0.60562925	-4.738821465	-0.52317076	3.301251956
380	188.5	37.1	4.457	0.656020018	3.28994564	0.647517152	-3.515784815	-0.525437561	2.688498001
420	191.5	39.4	3.565	0.524727701	3.342305518	0.687659725	-2.699491862	-0.549217827	2.26281428
460	190.5	43.4	2.416	0.355607889	3.324852225	0.757472895	-1.726009996	-0.319897044	1.660003426
500	190	43.7	1.983	0.291875184	3.316125579	0.725147474	-1.411863579	-0.248949642	1.370019821
530	189.4	43	1.796	0.264350898	3.305653603	0.750491578	-1.295873631	-0.214530489	1.224869055
560	192.6	46.8	1.213	0.178539888	3.361504139	0.81681409	-0.810357987	-0.181136471	0.884238945
590	258	68.2	0.0755	0.011112747	4.50294947	1.19031455	-0.005829484	-0.027425568	0.07010068
Qam									
125	D	I	J(Am <sup>2</sup> /Kg) e <sup>-3</sup>	J/J0	Drad	Irad	X	Y	Z
20	47.3	14.5	2.118	1	0.825540736	0.253072742	1.390591293	1.50696935	0.530304849
100	47	12.8	1.996	0.942398489	0.820304748	0.223402144	1.32744032	1.423505463	0.442210801
140	48.6	12.6	1.691	0.798394712	0.848230016	0.219911486	1.0913466	1.237889729	0.368880221
180	45.1	12.4	1.456	0.687440982	0.787143493	0.216420827	1.003773964	1.007283926	0.312654636
220	45.2	13.2	1.261	0.595372993	0.788888822	0.230383461	0.865067438	0.871127928	0.287950447
260	41.1	12.8	1.123	0.530217186	0.717330323	0.223402144	0.825221789	0.719886849	0.248798963
300	37.4	12.9	0.928	0.438149197	0.65275314	0.225147474	0.718610297	0.549419058	0.207176108
340	37.1	15.4	0.8221	0.388149197	0.647517152	0.268780705	0.632151329	0.478092295	0.218313684
380	37.1	15.2	0.7106	0.335505194	0.647517152	0.265290046	0.546935778	0.41364428	0.18631163
420	34.2	17	0.5839	0.275684608	0.596902604	0.296705973	0.461830501	0.313859684	0.170715838
460	17.5	21.2	0.2915	0.137629839	0.305432619	0.37009801	0.259193933	0.081723533	0.105413562
500	1.1	23.7	0.1901	0.089754485	0.019198622	0.413643033	0.17403538	0.00334165	0.076410272
530	342.3	25.1	0.1456	0.068744098	5.97426203	0.438077642	0.125609195	-0.040087008	0.061763436
560	326.3	25.1	0.1099	0.051888574	5.695009349	0.438077642	0.082797747	-0.055219233	0.046619517
590	309.8	23.4	0.01152	0.005439093	5.407030023	0.408407045	0.006767581	-0.008122703	0.004575144

Table 7) Continued.

Qam 271	D	I	J(Am <sup>2</sup> /Kg) e <sup>-4</sup>	J/J0	Drad	Irad	X	Y	Z
	6.7	55.1	10.04	1	0.11693706	0.961676418	5.705114427	0.670196915	8.234324834
	5.8	55.3	8.88	0.884462151	0.101229097	0.965167076	5.029323116	0.510860013	7.300639084
	6.5	58.7	7.492	0.746215139	0.113446401	1.024508271	3.867217324	0.440613758	6.401605555
	9	61.7	6.302	0.627689243	0.157079633	1.076868148	2.950920301	0.46737986	5.548768282
	11.1	63	4.672	0.465338645	0.193731547	1.099557429	2.081364539	0.408347488	4.162782481
	8.3	62.1	3.304	0.329083665	0.144862328	1.083849465	1.529846556	0.223180476	2.919961642
	358.2	59.8	1.471	0.146513944	6.251769381	1.043706893	0.739577225	-0.023242151	1.271348234
	358.3	59.3	1.759	0.175199203	6.25351471	1.034980246	0.897649727	-0.026641622	1.512480146
	8.4	60.1	2.26	0.225099602	0.146607657	1.04894288	1.114496692	0.164574553	1.959186653
	1	61.5	2.248	0.223904382	0.017453293	1.07337749	1.072489523	0.018720374	1.975580869
	2.8	63.9	1.028	0.102390438	0.048869219	1.115265392	0.451717533	0.022092673	0.923172348
	4	72.8	0.4958	0.04938247	0.06981317	1.270599695	0.146254912	0.01022714	0.473627012
	351.4	70.2	0.4053	0.040368526	6.133086992	1.225221135	0.135746837	-0.020529779	0.381338976
	349.6	71.3	0.2292	0.022828685	6.101671065	1.244419757	0.072277255	-0.013265359	0.217100596
	298.2	17.2	0.03113	0.003100598	5.204571829	0.300196631	0.014052627	-0.026208039	0.009205392
Qam 381	D	I	J(Am <sup>2</sup> /Kg) e <sup>-3</sup>	J/J0	Drad	Irad	X	Y	Z
	175.4	26.1	2.368	1	3.061307508	0.455530935	-2.11967949	0.170545362	1.041775954
	174.7	25.3	2.329	0.983530405	3.049090203	0.441568301	-2.096606147	0.194496272	0.995316464
	175.8	24.8	2.218	0.936655405	3.068288825	0.432841654	-2.00804328	0.147461481	0.930344719
	177.1	25.3	2.113	0.892314189	3.090978105	0.441568301	-1.907879982	0.09664903	0.903007165
	176.7	25.1	1.997	0.843327703	3.083996788	0.438077642	-1.805422198	0.104099989	0.847126247
	173.8	25.4	1.917	0.809543919	3.03338224	0.44331363	-1.721565017	0.18702181	0.822268651
	173	26.1	1.798	0.759290541	3.019419606	0.455530935	-1.602618198	0.196776772	0.791010627
	176.4	25.8	1.712	0.722972973	3.078760801	0.450294947	-1.538304243	0.0967819	0.745115642
	174	26	1.605	0.677787162	3.036872898	0.453785606	-1.434661925	0.150789045	0.703585691
	177.9	26.2	1.496	0.631756757	3.104940739	0.457276264	-1.341397025	0.049186796	0.660492756
	181.5	25.5	1.16	0.489864865	3.167772592	0.445058959	-1.046640149	-0.027407237	0.499392872
	180.5	26.4	0.7476	0.315709459	3.1503193	0.460766923	-0.669608614	-0.005843586	0.33240926
	179.4	26.1	0.4255	0.1796875	3.131120678	0.455530935	-0.382089782	0.004001381	0.187194117
	182.1	27.1	0.1677	0.070819257	3.178244568	0.472984227	-0.149188424	-0.005470491	0.076394881
	188	31	0.01653	0.006980574	3.281218994	0.541052068	-0.014031084	-0.00197194	0.008513579

Table 8) Results of applying Krichsvink analysis on specimen Asi 131 to determine the number of linear segments and demagnetisation planes of component magnetisations and their directions.

Directions which pass 5.0 Degree Linearity Test								
SAMPLE	DEMAG.STEPS	GDEC	GINC	SDEC	SINC	INT	PTS	ERR.ANG.
Asi 131	530 to 560	252.6	77.6	252.6	77.6	7.68E+04	3	2.2
Asi 131	300 to 560	216.3	81.7	216.3	81.7	1.10E+06	9	1.5
Asi 131	140 to 260	17.2	85.4	17.2	85.4	3.23E+05	4	2
No more linear segments.								
Normal vectors to least-square demag.planes:A.S.D. less than 5.0								
SAMPLE	DEMAG.STEPS	GDEC	GINC	SDEC	SINC	PTS	ERR.ANG	
Asi 131	460 to 560	319.8	-5	319.8	-5	5	3.9	
Asi 131	140 to 530	302.1	0.4	302.1	0.4	11	5	
Asi 131	100 to 220	150.6	1.6	150.6	1.6	4	1.2	
No more demagnetisation planes.								

**4- Changes in the direction of remanent magnetisation**

During the demagnetisation experiments, progressive changes occur in both intensity and

direction of remanent magnetisation. In the previous section, the change in the intensity of magnetisation of the pilot samples was reported. In this section the trend of change in the direction of magnetisation would be examined

by plotting demagnetisation results on orthogonal diagrams (Zijderveld Diagrams).

The calculated x, y, and z values (Table 7) have been used to construct Zijderveld Diagrams or Z-plots that illustrate changes in the directions of magnetisation during the demagnetisation process for five thermally demagnetised pilot samples: Asi 131, Asi 184, Qam 125, Qam 271 and Qam 381. In the final analysis, i.e. the

stage that corresponds to the last thermal demagnetisation step at 590° C is dropped because it is higher than the Curie temperature of Magnetite (580° C).

The plotted Zijderveld diagrams for the five pilot samples are shown in Figs.10, 11, 12, 13 and 14. For Jisr el Asi locality no tilt correction has been made, therefore the indicated directions are in situ results.

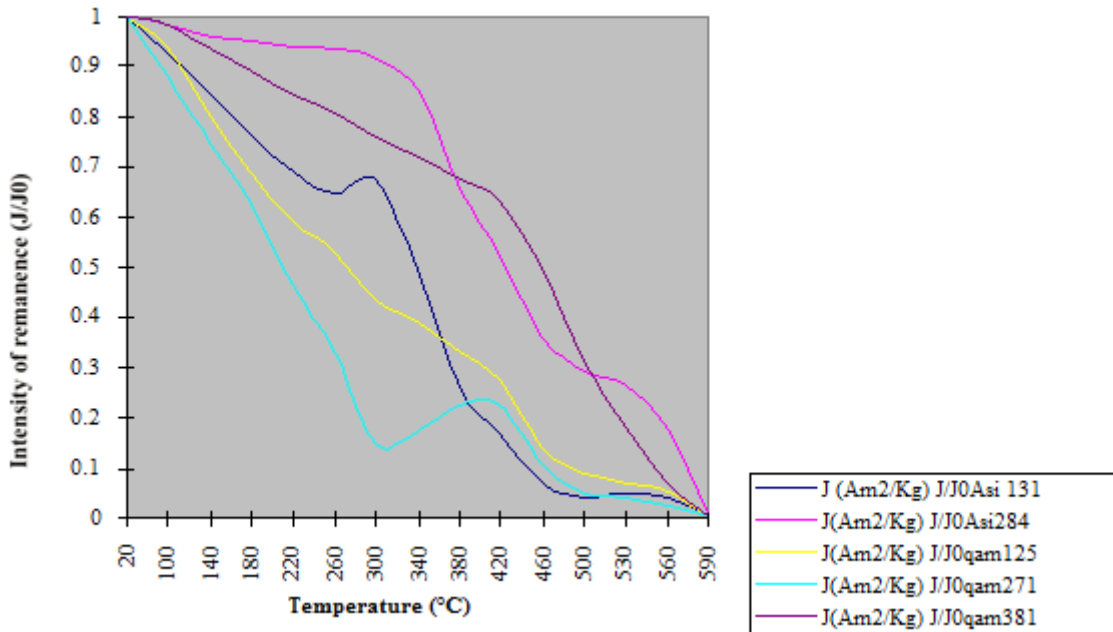


Figure 8) Decay of Intensity during demagnetisation. Progressive Thermal demagnetisation curves of five pilot specimens. Variation in the pattern of behavior of individual samples is evident and indicates the presence of multi-component system. This shows that identical hand specimens can have different magnetic composition.

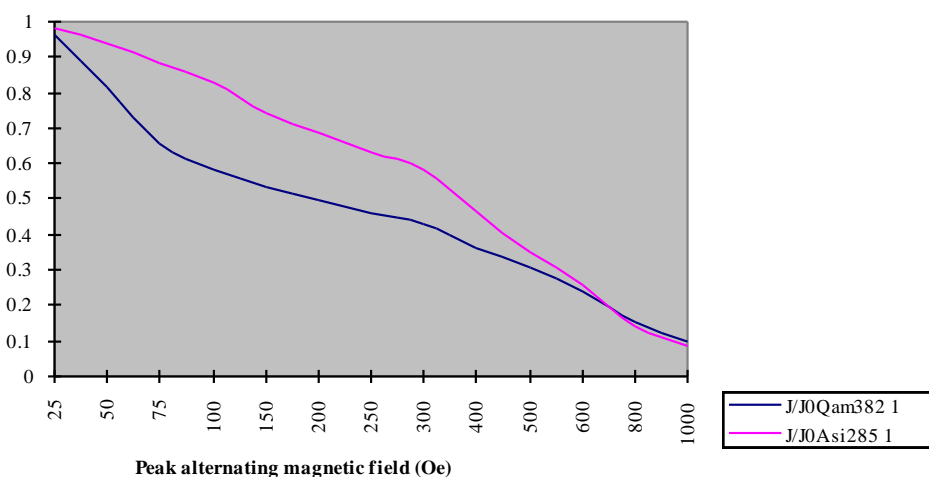


Figure 9) Decay of intensity during demagnetisation. Alternating field demagnetisation curves of two pilot basalt samples, one from each locality. Note how remanence is very stable against AF cleaning. Such high stability against AF is characteristic of thermal remanent magnetisation (TRM). The plot points to 1000-2000 Oe coercivity of remanence.

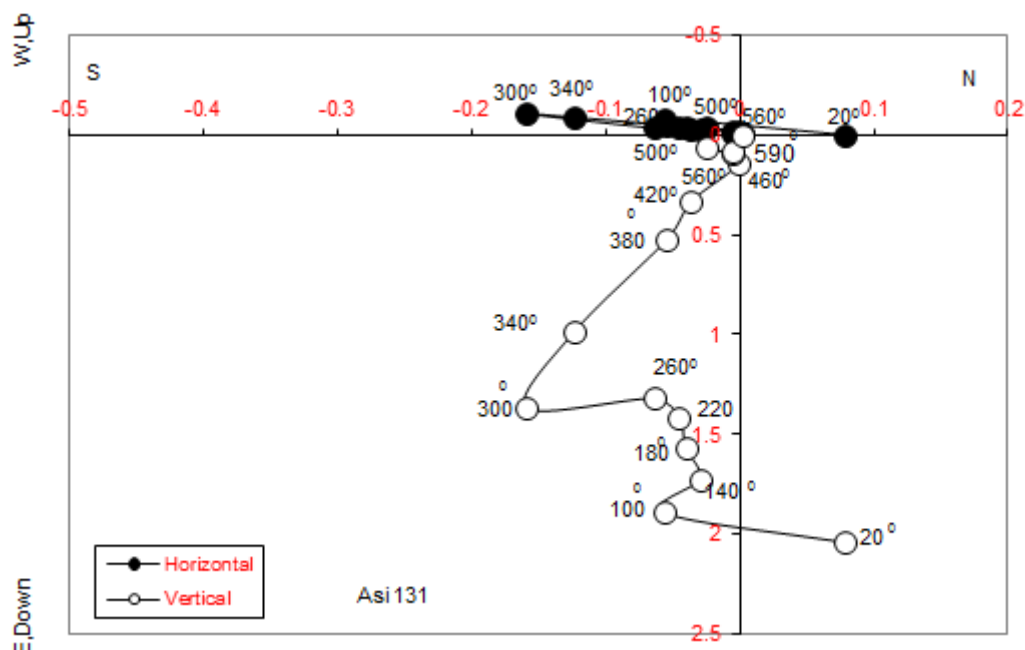


Figure 10) Vector demagnetisation diagram (Zijderveld plot) of specimen Asi 131. Solid circles are projections of the magnetic vector that lie on the horizontal plane and open circles are projections onto the N-S vertical plane.

In the above diagram, by excluding the last value (corresponding to  $590^{\circ}$  C) because it is above the Curie point of Magnetite ( $580^{\circ}$  C), the declination is southward. The inclination is downward and steep. In the demagnetisation process different system components are represented in Z-plots by different straight line segments. From this it can be seen that the plot exhibits some complexity due to multiphase composition (presence of various straight segments) and phase overlap (the connecting small curves between successive segments). This feature has also been indicated previously by our explanation for the change of intensity of magnetisation in thermal cleaning (Fig. 8). In this regard should be mentioned that the larger overlap of coercivity or blocking temperatures between the interlacing components the harder will be their isolation during the demagnetisation process. Because of this and also because that a certain amount of coercivity overlapping doesn't necessarily mean that blocking temperature overlapping has the same range, it becomes clear that proper choice of cleaning method (A.F. or thermal) is critical.

The straight line segments can be used to calculate the primary direction of magnetisation (Verosub, 2000). However in complex multi-phase system discrimination or separation between primary and secondary directions is not a straight-forward procedure. Therefore it is desirable to have an estimate of the direction of the principal component of magnetisation and average direction of remanence from the various linear segments. In the present study, the estimation of directions of linear segments in the z-plots, original complex multivariate technique of Kirschvink (Kirschvink, 1980) is followed by the use of special software (x, y, z) for DOS. Because the precision of the segment lines that best fit along various demagnetisation paths in Zijderveld diagram is determined by MAD (maximum angular deviation) and since MAD values of  $\sim 10^{\circ}$  would yield better results (MacEilhiny and MacFadden, 2000), therefore a MAD value of  $5^{\circ}$  is adopted. The following table (Table 8) shows the results obtained for specimen Asi 131.

From the Table 8 it can be observed that for sample Asi 131 there are three linear segments in the intervals denoted above along with the

indicated inclinations and declinations. The average direction of these three components would then be 162° for the declination and 81.6° for inclination. Though such combination of

southward declination and downward (positive) inclination is interpreted here to indicate transitional /Intermediate polarity, the very steep inclination is queer in this context.

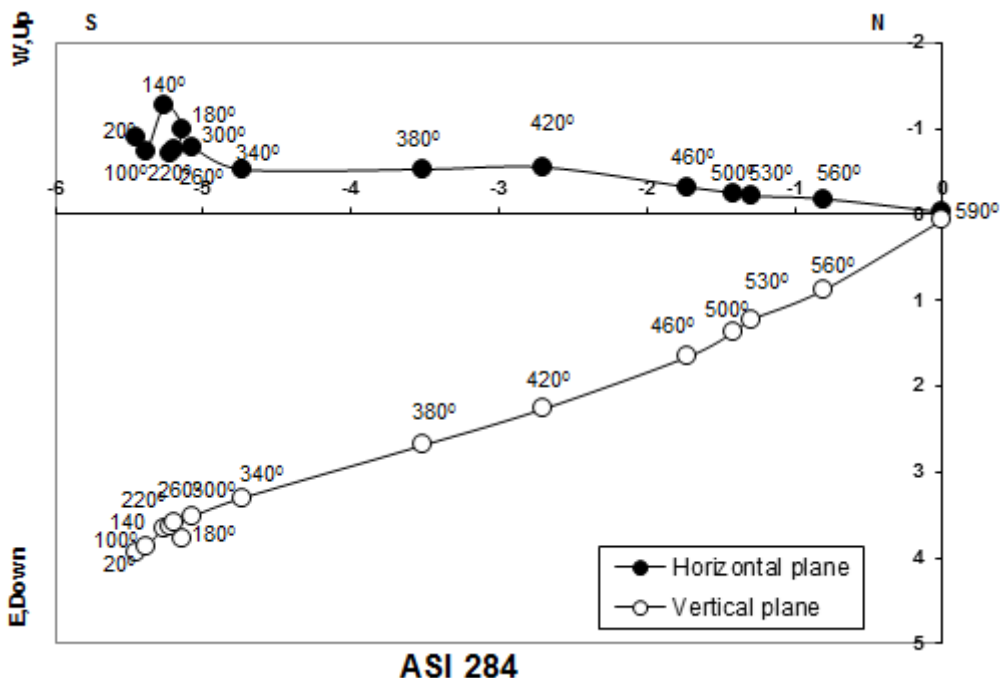


Figure 11) Vector demagnetisation diagram (Zijderveld plot) of specimen Asi 284. Solid circles are projections of the magnetic vector that lie on the horizontal plane and open circles are projections onto the N-S vertical plane. It is clear that softer or secondary magnetisation are progressively eliminated in the range up to 3000 C where the curve shows successive directional changes until finally the primary/characteristic component is isolated (see later note on the result of Kirschvink analysis of this sample).

In the Figure 11, once more for Al-Asi basalt locality, the z-plot of the other specimen, Asi 284, is shown. The declination is southward while inclination is down (positive), however, the inclination is moderate and unlike the

anomalous steep values of specimen Asi 131. For defining the linear segments in the z-plots, Kirschvink analysis is again applied. The results are shown in Table 9.

Table 9) Results of applying Kirschvink analysis on specimen Asi 284 to determine the number of linear segments and demagnetisation planes of component magnetisations and their directions.

Directions which pass 5.0 degree Linearity Test								
SAMPLE	DEMAG.STEPS	GDEC	GINC	SDEC	SINC	INT	PTS	ERR.ANG.
ASI 284	140 TO 560	189.4	35.5	189.4	35.5	5.23E+06	13	4.8
(No more linear segments)								
Normal vectors to least-squares demag.planes: A.S.D. less than 5.0								
SAMPLE	DEMAG.STEPS	GDEC	GINC	SDEC	SINC	PTS	ERR.ANG	
Asi 284	500 to 560	78.2	21.2	78.2	21.2	4	0.5	
Asi 284	500 to 560	78.3	21.2	78.3	21.2	4	0.4	
Asi 284	420 TO 530	102.2	1.5	102.2	1.5	4	3.1	
Asi 284	340 TO 460	42.3	55.2	42.3	55.2	4	4.3	
Asi 284	260 TO 420	197.8	-61.8	197.8	-61.8	5	3.1	
(No more demagnetisation planes)								

A good analogy can be seen between the behaviour of this curve and that shown in Figure 8 where blocking temperature lies in the range

340-580° C. Application of Kirshsvink analysis Shows simpler component entity (in comparison to that of specimen Asi 131) where only one

single linear segment is defined (within 5.0 degree linearity test) having  $189.4^\circ$  declination and  $35.5^\circ$  inclination. Thus by this southward declination and downward (positive) inclination a transitional direction/intermediate polarity is indicated. This general behaviour is similar to that of specimen Asi 131 though the latter has anomalous steep inclination. Next, the z-plots and associated Kirschvink analysis were performed on specimens from the southern Al Qamoua locality.

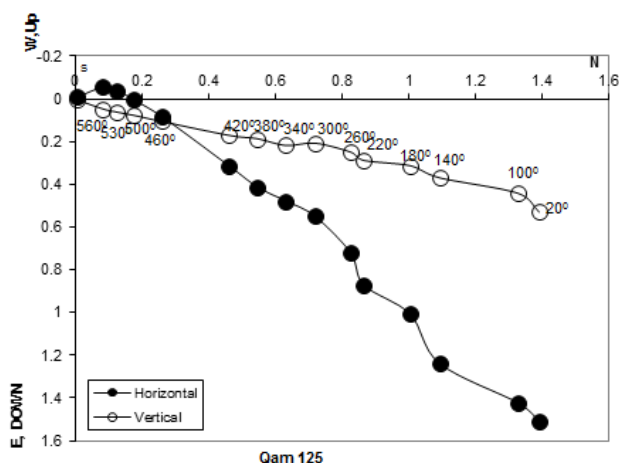


Figure 12) Vector demagnetisation diagram (Zijderveld plot) for Qam 125 specimen. Solid circles are projections of the magnetic vector that lie on the horizontal plane and open circles are projections onto the N-S vertical plane. The plot assumes simple component entity that has been also reflected previously in the demagnetisation curve of Figure 8 for the same specimen. This feature will be stressed once more by Kirschvink analysis as shown hereafter.

In the Figure 12, a northward declination and low-moderate down (positive) inclination is indicated for specimen Qam 125. This feature of the inclination differs from the other, previously described, specimens of the northern Al-Asi basalt locality. Applying Kirschvink analysis on this thermally demagnetised specimen provided the following data (Table 10).

This analysis shows that the identified linear segment includes the entire analysed spectrum (principal uni-phase) with northward declination

of  $45.1$  and downward (positive) inclination of low-intermediate value of  $13.5$ . This clearly defines Normal Polarity for the first site of Al-Qamoua locality (Qs1). The z-plot for the second specimen (Qam 271) from the southern Al Qamoua locality is shown in Figure 13.

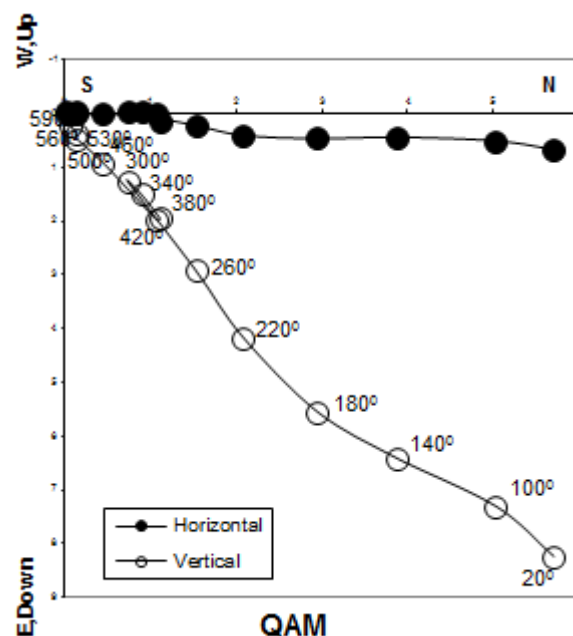


Figure 13) Vector demagnetisation diagram (Zijderveld plot) for Qam 271 specimen. Solid circles are projections of the magnetic vector that lie on the horizontal plane and open circles are projections onto the N-S vertical plane.

In the Figure 13, the simple component behaviour becomes complicated by the appearance of another phase of opposite (reversed) declination and inclination (declination  $207.3$  and negative inclination of  $-58.8$ ) in the  $300^\circ$  to  $380^\circ$  interval (compare with the “bump” for this same interval as shown in the curve of this specimen; Fig. 8). It is difficult to speculate on this minor component. Lightning effects or self-reversal may be invoked as possible explanations. In general, the specimen shows northward declination and down (positive) steeper inclination than that of specimen Qam 125. Applying Kirschvink analysis on this thermally demagnetised specimen provided the following results (Table 11).

Table 11) Kirschvink analysis results for specimen Qam 271 that provide the identified number of linear segments and demagnetisation planes of component magnetisation and their directions.

<b>Directions which pass 5.0 degree Linearity Test</b>								
SAMPLE	DEMAG.STEPS	GDEC	GINC	SDEC	SINC	INT	PTS	ERR.ANG.
QAM 271	380 to 560	4.4	61.6	4.4	61.6	1.81E+06	7	3.5
QAM 271	300 to 380	207.3	-58.8	207.3	-58.8	6.44E+05	3	2.4
QAM 271	180 to 260	9.5	61.1	9.5	61.1	2.40E+06	3	2.8
QAM 271	20 to 220	3.4	46.7	3.4	46.7	4.37E+06	5	4
No more linear segments								
<b>Normal vectors to least-squares demag.planes: A.S.D. less than 5.0</b>								
SAMPLE	DEMAG.STEPS	GDEC	GINC	SDEC	SINC	PTS	ERR.ANG	
Qam 271	180 to 300	236	21	236	21	4	4.5	
No more demagnetisation planes.								

Table 12) Kirschvink analysis results for specimen Qam 381 that provides the identified number of linear segments and demagnetisation planes of component magnetisation and their directions.

<b>Directions which pass 5.0 degree Linearity Test</b>								
SAMPLE	DEMAG.STEPS	GDEC	GINC	SDEC	SINC	INT	PTS	ERR.ANG.
Qam 381	220 to 560	175.8	25.7	175.8	25.7	1.60E+06	11	4.1
QAM 381	20 to 180	177.7	2.7	177.7	2.7	1.55E+06	4	2.8
No more linear segments.								
<b>Normal vectors to least-squares demag.planes: A.S.D. less than 5.0</b>								
SAMPLE	DEMAG.STEPS	GDEC	GINC	SDEC	SINC	PTS	ERR.ANG	
Qam 381	500 to 560	39.7	57.3	39.6	57.4	4	3.3	
Qam 381	500 to 560	44	55.5	44	55.5	4	2.7	
Qam 381	220 to 340	155.8	-68.4	155.8	-68.4	4	4.9	
Qam 381	100 to 220	88.7	-29.4	88.7	-29.4	4	2.9	
No more demagnetisation planes								

This analysis shows that the identified linear segment includes the entire analysed spectrum (principal uni-phase) with northward declination of 45.1 and downward (positive) inclination of low-intermediate value of 13.5. This clearly defines Normal Polarity for the first site of Al-Qamoua locality (Qs1). The z-plot for the second specimen (Qam 271) from the southern Al Qamoua locality is shown in Figure 13.

In the Figure 13, the simple component behaviour becomes complicated by the appearance of another phase of opposite (reversed) declination and inclination (declination 207.3 and negative inclination of -58.8) in the 300° to 380° interval (compare with the “bump” for this same interval as shown in the curve of this specimen, Fig. 8). It is difficult to speculate on this minor component. Lightening effects or self-reversal may be invoked as possible explanations. In general, the specimen shows northward declination and down (positive) steeper inclination than that of

specimen Qam 125. Applying Kirschvink analysis on this thermally demagnetised specimen provided the following results (Table 11).

This analysis indicates that except for the minor component that appears in the interval 300° to 380° C, the identified linear segments of the specimen show northward declination averaging 5.80 and downward (positive) inclination averaging 56.50. This defines Normal Polarity for the second site of Al-Qamoua locality (Qs2).

Finally, the z-plot for the third specimen (Qam 381) from the southern Al Qamoua locality is shown in Figure 14.

The above z-plot for specimen Qam 381 indicates southward declination and downward-positive inclination. This transitional direction is different from the other two sites of the Al-Qamoua locality specimens (Qam 125 and Qam 271) and is similar to the direction revealed by the samples from of Al-Asi locality.

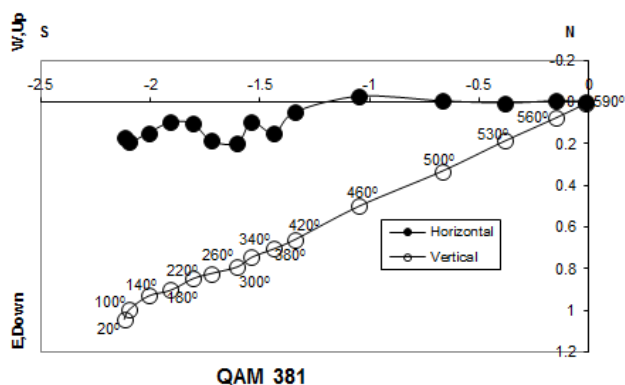


Figure 14) Vector demagnetisation diagram (Zijderveld plot) of specimen Qam 381. Solid circles are projections of the magnetic vector that lie on the horizontal plane and open circles are projections onto the N-S vertical plane.

Applying Kirschvink analysis on this thermally demagnetised specimen yielded the following results (Table 12).

Kirschvink analysis identifies two linear segments one for the interval 20 to 180° C and the other between 220 to 560° C. The average direction of both linear segments is a southward 176.8° declination and downward (positive) 140° inclination. These results define transitional/intermediate polarity. This separates the site of Tell Abu Tineh (Qs3) from the other two sites of Al-Qamoua locality (Qs1 and Qs2) and groups it with Al-Asi locality (As), however it has lower inclination than the value for both Asi 131 and Asi 284. This is feasible also from the provisional field geologic observations since Tell Abu Tineh site (specimen Qam 381) is located on the boundary between Al Qamoua locality and Al Asi locality. However, the reader is reminded that the provisional geological mapping conducted in the present research needs further data (large-scale mapping) to clarify the precise geologic relationship between these two effusive suites.

Summing up, the overall results from both Zijderveld diagrams and the associated Kirschvink analyses suggest that there are two basalt bodies representing two different volcanic outpourings:

The first is characterized by transitional direction/(intermediate) polarity with southward declination and down (positive) inclination. This is represented by the basalts of the northern (As) locality and one (Qam 3) northernmost sampling site from the southern (Qs) basalt locality. The second is characterized by Normal Polarity with northward declination and down (positive) inclination. This is represented by the two southern basalt sampling sites (Qam 1 and Qam 2). These results confirm the initial conclusion on polarity of the samples gained from non-cleaned NRM data (Figs. 5, 6 and 7).

## 5- Magnetic Susceptibility

Magnetic susceptibility in rocks is related to the magnetic content of the rock; specifically the amount, shape and composition of the magnetic minerals (Nagata, 1967; Tarling and Hrouda, 1993). Magnetic susceptibility is considered an indicator for the degree of magnetic anisotropy of rocks hence it is important in determining the reliability of NRM. Anisotropy of magnetisation, in terms of foliation and lineation parameters, leads to deviation in the alignment of primary magnetisation from that of the ambient field and the appearance of scatter in the observed directions of magnetisation. For measuring the bulk magnetic susceptibility of the basalt samples in the current study a susceptibility bridge KLY-3 and software SUSAR version 1.4 were used. Average weights of specimens are recorded in Tables 3 and 4. The most importantly measured parameters are shown in Table 13.

Variation of susceptibility at the successive thermal demagnetisation steps is shown in Figure 15.

Table 13) The most important parameters of susceptibility measurements of five thermally demagnetised pilot samples (ASI 131, ASI 184, QAM 125, QAM 271 and QAM 381). Volume of specimens ( $v$ ) = 11.70 (for volume susceptibility). The  $k$ ,  $L$ ,  $F$ ,  $P$  and  $T$  represent susceptibility, lineation, foliation, degree of anisotropy and shape parameter.

ASI131							ASI284						
T (°C)	K e-3	L	F	P	T	K/KO	K e-3	L	F	P	T	K/KO	
20	2.22	1	1	1.01	0.33	1	9.79	1.01	1	1.01	-0.4	1	
100	2.33	1	1.01	1.01	0.58	1.051351	9.91	1.01	1	1.01	-0.3	1.012874	
140	2.52	1	1.01	1.01	0.5	1.133333	10.2	1.01	1	1.01	-0.3	1.045264	
180	2.67	1.01	1.01	1.02	0.42	1.204054	10.5	1.01	1	1.01	-0.3	1.072852	
220	2.7	1.01	1.01	1.02	0.41	1.216667	10.7	1.01	1	1.01	-0.2	1.092265	
260	2.76	1	1.01	1.02	0.51	1.240991	10.8	1.01	1	1.01	-0.2	1.105548	
300	2.81	1.01	1.02	1.02	0.44	1.264414	11	1.01	1	1.01	-0.3	1.121896	
340	3.05	1.01	1.02	1.03	0.41	1.375676	11.1	1.01	1	1.01	-0.1	1.138245	
380	4.27	1.01	1.02	1.03	0.48	1.924775	11.3	1.01	1	1.01	-0.2	1.156636	
420	8.62	1.01	1.02	1.03	0.4	3.883784	11.7	1.01	1	1.01	-0.3	1.191376	
460	33.9	1.01	1.02	1.03	0.32	15.26577	14.5	1	1	1.01	-0.1	1.476448	
500	34.2	1.01	1.02	1.02	0.39	15.3964	15.6	1	1	1.01	-0.2	1.593951	
530	32.8	1.01	1.01	1.02	0.36	14.79279	16.4	1	1	1.01	-0.2	1.673649	
560	31.2	1.01	1.01	1.02	0.4	14.04955	15.8	1	1	1.01	-0.2	1.612343	
590	25.4	1	1.01	1.01	0.65	11.45045	14.1	1	1	1.01	-0.2	1.438643	
QAM125							QAM271						
T (°C)	K e-3	L	F	P	T	K/KO	k e-3	L	F	P	T	K/KO	
20	6.08	1.03	1.03	1.06	0.07	1	2.75	1.01	1.01	1.02	0.15	1	
100	6.65	1.03	1.04	1.07	0.09	1.093796	3.13	1.01	1.01	1.02	0.2	1.136265	
140	7.07	1.03	1.04	1.07	0.19	1.162909	3.21	1.01	1.01	1.02	0.26	1.166424	
180	7.26	1.03	1.05	1.08	0.23	1.195327	3.18	1.01	1.01	1.02	0.27	1.155887	
220	7.36	1.03	1.05	1.08	0.28	1.210959	3.22	1.01	1.01	1.02	0.21	1.170785	
260	7.4	1.03	1.05	1.08	0.31	1.218035	3.23	1.01	1.01	1.02	0.28	1.172602	
300	7.41	1.02	1.05	1.08	0.37	1.219023	3.22	1.01	1.01	1.02	0.43	1.170785	
340	7.92	1.03	1.06	1.08	0.38	1.303933	4.03	1.01	1.01	1.02	0.46	1.464753	
380	9.31	1.03	1.07	1.1	0.35	1.531512	6.99	1.01	1.02	1.03	0.45	2.541424	
420	10.5	1.03	1.08	1.11	0.42	1.727826	10.2	1.01	1.02	1.03	0.51	3.69186	
460	9.47	1.03	1.07	1.09	0.45	1.558828	8.36	1	1.02	1.02	0.72	3.039244	
500	8.56	1.02	1.06	1.08	0.5	1.409083	7.92	1	1.02	1.02	0.86	2.87609	
530	7.62	1.01	1.05	1.07	0.55	1.25325	7.39	1	1.01	1.02	0.74	2.68641	
560	6.95	1.01	1.04	1.05	0.6	1.142834	7.06	1	1.01	1.01	0.29	2.565044	
590	5.79	1.01	1.03	1.04	0.71	0.95195	5.83	1	1	1.01	-0.3	2.118823	
QAM381													
T (°C)	k e-3	L	F	P	T	K/KO							
20	15	1.01	1.02	1.03	0.45	1							
100	15.1	1.01	1.02	1.03	0.47	1.010027							
140	15.3	1.01	1.02	1.03	0.44	1.024064							
180	15.5	1.01	1.02	1.03	0.44	1.038102							
220	15.7	1.01	1.02	1.03	0.45	1.04746							
260	15.8	1.01	1.02	1.03	0.5	1.052807							
300	15.8	1.01	1.02	1.03	0.46	1.054813							
340	15.8	1.01	1.02	1.03	0.53	1.058824							
380	15.8	1.01	1.02	1.03	0.53	1.057487							
420	15.7	1.01	1.02	1.03	0.49	1.052139							
460	15.4	1.01	1.03	1.03	0.58	1.027406							
500	14.9	1.01	1.02	1.03	0.58	0.995321							
530	14.4	1.01	1.02	1.03	0.59	0.960561							
560	14	1.01	1.02	1.03	0.55	0.933155							
590	13.3	1.01	1.02	1.03	0.53	0.891043							

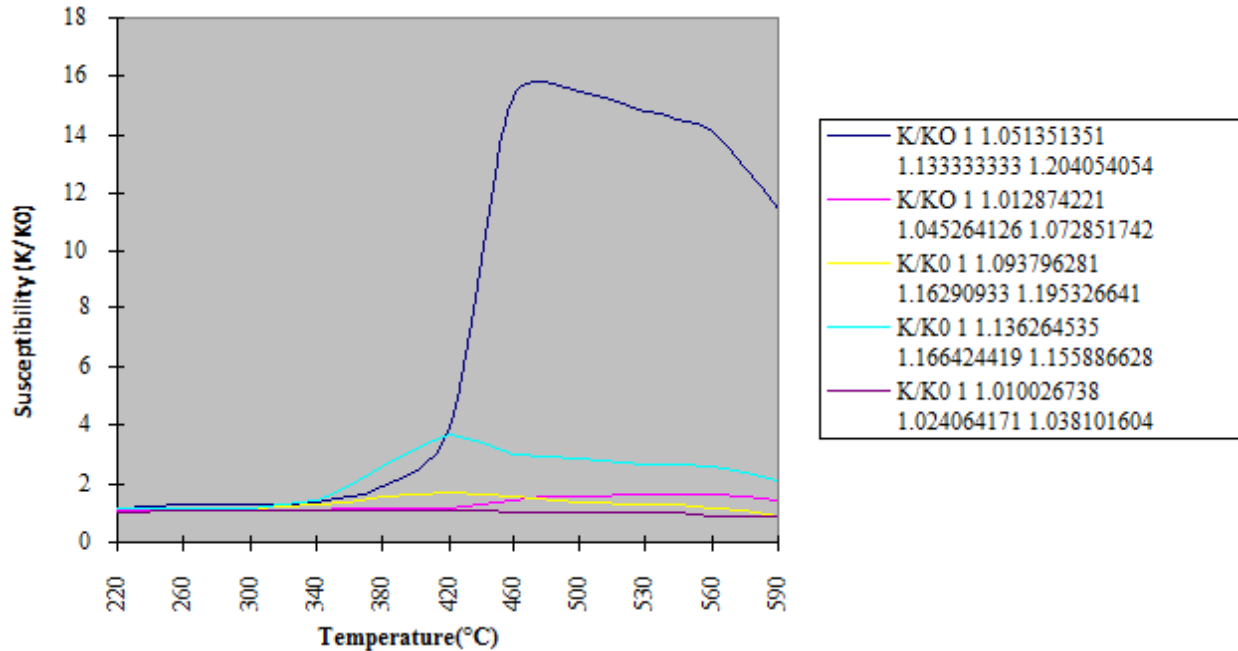


Figure 15) Susceptibility changes (at room temperature) during progressive thermal demagnetisation of five pilot samples. Note that specimen asi 131 shows abrupt increase in the interval 400°C - 460°C followed by steady decrease with two deflection points one at 480°C and the other at 500°C denoting significant chemical alteration of the sample (hence a change in its magnetic properties). Sample Qam 271 shows but lesser change in the interval 340°C-420°C reflecting some degree of mineralogic change. The other three samples show negligible or very small change in the course of successive heating.

## 6- Anisotropy of Magnetisation

In palaeomagnetic work, an important issue is to check the degree of representation of the measured remanence to the direction of the ancient ambient field. This can be achieved by determining the anisotropy of magnetisation. The anisotropy in rocks is related to the shape of the constituent minerals and their alignment. It can also be produced after the acquisition of remanence as a result of external factors such as stress effects (tectonic and non-tectonic). For this reason magnetic anisotropy represents also a magnetic method to determine the petrofabrics of rocks and the evaluation of the strain evolution and strength of all rock types (Tarling and Hrouda, 1993). The

higher the anisotropy the lesser parallelism would be. If the limit of 5% is exceeded then divergence should be considered significant (Irving, 1964). One of the magnetic methods to determine the anisotropy is by measuring the variation in susceptibility (Girdler, 1961). Thus, maximum, intermediate and minimum susceptibility values define the three principal axes of triaxial ellipsoid (or susceptibility ellipsoid) that portrays the susceptibility anisotropy of a rock sample (Irving, 1964; Tarling and Hrouda, 1993).

In thermal remanent magnetisation (TRM), if the rock is anisotropic then the acquired magnetisation during the cooling process would not be exactly parallel to the ambient field but it would be deflected in the direction of maximum anisotropy “the easy direction”. The larger value of the

anisotropy, the more deflection from the ambient field.

For sample ASI 131:  $K_1=1.000$ ,  $K_2=1.003$  and  $K_3=0.909$  Where  $K_1$ ,  $K_2$  and  $K_3$  are the principal susceptibilities (maximum, intermediate and minimum respectively) of the sample in SI units. The declination (D) and inclination (I) of the above maximum ( $K_1$ ), intermediate ( $K_2$ ) and minimum ( $K_3$ ) principal susceptibilities are 144/21, 330/60, and 236/5 respectively. The calculated average values of different anisotropy parameters are:  $L=1.005$ ,  $F=1.014$ ,  $P=1.019$ ,  $T=0.435$  and  $q = 0.331$ , where  $L$ ,  $F$ ,  $P$ , and  $T$  and  $q$  correspond to magnetic lineation, magnetic foliation, prolateness and shape parameters respectively. Both  $T$  and  $q$  (shape parameters) are calculated in two different ways where  $q$  follows Granar formula (Granar, 1958).

For sample QAM 125:  $K_1 = 1.032$ ,  $K_2 = 1.000$  and  $K_3=0.960$ . The declination (D) and inclination (I) of the above maximum ( $K_1$ ), intermediate ( $K_2$ ) and minimum ( $K_3$ ) principal susceptibilities are 106/39, 336/38

and 350/28 respectively. The calculated average values of different anisotropy parameters are:  $L=1.023$ ,  $F=1.050$ ,  $P=1.075$ ,  $T=0.362$  and  $q=0.391$ .

The interest is to observe the degree of anisotropy of magnetic susceptibility (AMS), hence the degree of deflection of the acquired magnetisation from the ambient field. The degree of anisotropy or the anisotropy factor (in terms of susceptibility) according to Irving (1964), Nagata (1967) and MacElhinny and MacFadden (2000) is defined as:

$A_n = X_{max} / X_{min}$ . From Table 13 and the values of the two stereographic plots, the degree of anisotropy of the five demagnetised pilot samples is:  $A_n = 1.01$  for both ASI 131 and ASI 284,  $A_n = 1.08$  for QAM 125,  $A_n = 1.02$  for QAM 271 and  $A_n = 1.03$  for QAM 381.

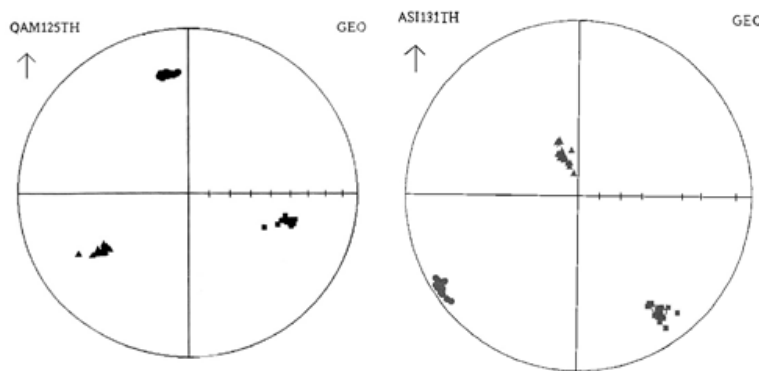


Figure 16) Stereographic-polar projection of the anisotropy directional data. Solid squares correspond to direction of maximum principal axis, solid triangles for the direction of the intermediate principal axis and solid circles stand for the minimum principal axis. As observed in these two projections, the directions form three separate groups, thus they define triaxial susceptibility ellipsoid. The most favourable case for the deflection of the TRM from the direction of the ambient field occurs when the applied earth magnetic field is along the plane of the maximum-minimum susceptibility.

The value  $An = 1.01$  means that maximum susceptibility exceeds the minimum by 1% which indicates that the sample has 1 percent anisotropy of magnetic susceptibility (for both samples from Al Asi locality). For the other three samples from Al-Qamoua locality we have 8% anisotropy for sample QAM 125, 2% anisotropy for sample QAM 271 and 3% anisotropy for sample Qam 381. Stereographic projection for the anisotropy directional data of two samples (ASI 131 and QAM 125) is shown on Figure 16.

It can be observed that the samples from Al-Qamoua locality show higher anisotropy than those of Al-Asi locality.

In the plane that contains both axes of maximum and minimum susceptibility (that is the favourable direction for the occurrence of deflection in the acquired magnetism when the direction of the applied field follows this path) consider that both the ambient magnetic field and TRM make angles  $\theta$  and  $\phi$  respectively with the axis of maximum susceptibility, then the relation of both angles to the degree of anisotropy ( $An$ ) can be written in equation form:

$$(\theta - \phi)_{\max} = \tan \left[ \frac{An - 1}{2 An} \right]$$

Accordingly, the anisotropy of susceptibility 1% (or  $An=1.01$ ) for the two samples of Al-Asi locality indicate that the maximum TRM deflection from the direction of the ambient field is less than  $1^\circ$  ( $0.63^\circ$ ). For the other three samples from Al-Qamoua locality the maximum deflections of the acquired magnetisation from the ambient field are as follows: sample QAM 125 (with anisotropy of susceptibility 8% or  $An=1.08$ ) the maximum deflection is  $5.7^\circ$ , for sample QAM 271 (with anisotropy of susceptibility 2% or  $An=1.02$ ) the maximum deflection angle is  $1.1^\circ$  and for sample QAM 381 (with anisotropy susceptibility 3% or  $An=1.03$ ) the maximum deflection angle is  $1.7^\circ$ .

Of importance in this regard is the limit of TRM deflection (or in other words the degree of

anisotropy) that is considered critical before the deviation from the ambient magnetic field becomes important. Irving (1964) considered a limit of anisotropy of about 5 percent (corresponding to degree of anisotropy  $An=1.05$ ) but he stated also that the effect of anisotropies of approximately 10% to 20 % (corresponding to deflections of  $5^\circ$  to  $10^\circ$  respectively) would be averaged out in certain circumstances. However, MacEllhinny and Macfaden (2000) are reluctant to consider a limit of 10% anisotropy (corresponding to degree of anisotropy  $An=1.1$ ) before significant divergence of TRM can occur. Therefore the calculated values for the angle of deflection of the five measured basalt samples of this study are all below the suggested limit and they occur within the tolerance range, hence the measured TRM directions are representative of the ambient field at the time of cooling of these basalts through their blocking temperature.

## 7- Correlation with the geomagnetic polarity time scale (mpts)

In a previous study, the present author has shown that the basalts of the present investigation have  $^{40}\text{Ar}/^{40}\text{Ar}$  age estimates of  $10.4 \pm 0.37$  Ma and  $10.87 \pm 0.31$  Ma (Lateef, 2014). Comparison of the gained polarity of the basalt samples with the Geomagnetic Polarity Timescale of Cande and Kent (1992; 1995) suggest that the palaeomagnetically investigated basalts are within the long  $\sim 1$  Myr (9.92-10.95 Myr) normal subchron C5n.2n. On the other hand, the transitional polarity probably corresponds to a cryptochron within C5n.2n (C5n.2n-1 to C5.2n-3).

## 8- Conclusions

The preliminary palaeomagnetic results of this paper indicate that the basalts from Al Asi location and from Qam 3 location belong to one volcanic flow characterized by transitional

polarity. Sites Qam 1 and Qam 3, on the other hand, belong to another volcanic emplacement that shows normal polarity. The normal component is correlated to the long normal polarity subchron C5n.2n while the transitional/intermediate component is possibly related to a cryptochron within C5n.2n.

### Acknowledgment

Considerable help and support was received from Dr. J. Hus, Director of the palaeomagnetism laboratory of the Centre of Physics of Earth, Dourbes, Belgium. The author is also thankful for Prof. Lisa Tauxe of University California, San Diego who read the manuscript and made encouraging comments. I also thank M.A. Ghanmi and an anonymous referee for their notes and evaluation on the submitted manuscript.

### References

- Cande, S. C., Kent, D. V. 1992. A new geomagnetic polarity time scale for the late Cretaceous and Cenozoic. *Journal of Geophysical Research*: 97, 13917–13951.
- Cande, S. C., Kent, D. V. 1995. Revised calibration of the geomagnetic polarity timescale for the late Cretaceous and Cenozoic. *Journal of Geophysical Research*: 100, 6093–6095.
- Girdler, R. W. 1961. Some preliminary measurements of anisotropy of magnetic susceptibility of rocks. *Geophysical Journal of the Royal Astronomical Society*: 5, 197–206.
- Granar, L. 1958. Magnetic measurements on Swedish varved sediments. *Arkiv för geofysik*: 3, 1–40.
- Gregor, C. B., Hertzman, S., Nairn, A. E. M., Megendank, J. 1974. The paleomagnetism of some Mesozoic and Cenozoic volcanic rocks from The Lebanon. *Tectonophysics*: 21, 375–394.
- Henry, B., Homberg, C., Mroueh, M., Hamdan, W., Higazi, F. 2010. Rotation in Lebanon inferred from new palaeomagnetic data and implications for the evolution of the Dead Sea Transform system. Homberg, C. and Bachmann, M. (Eds): *Evolution of the Levant Margin and Western Arabia Platform since the Mesozoic*. Geological Society, London, Special Publications: 341, 269–285.
- Irving, E. 1964, *Paleomagnetism and its application to geological and geophysical problems*, New York, John Wiley and Sons.
- Kirschvink, J. L. 1980. The least-square line and plane and the analysis of palaeomagnetic data. *Geophysical Journal of the Royal Astronomical Society*: 62, 699–718.
- Lateef, A. S. A. 2014. Miocene Volcanism in Lebanon Revealed By  $^{40}\text{Ar}/^{39}\text{Ar}$  Geochronology of Basalts from the North of the Bekaa Valley. *Journal of Advances in Geology*: 1, 1–12.
- McElhinny, M. W., McFadden, P. L. 2000. *Paleomagnetism: continents and oceans*, second ed. Academic Press, San Diego.
- Nagata, T. 1967. Rock magnetism. In Runcorn, S.K. (Ed.), *International dictionary of geophysics*. Pergamon Press, Oxford-London, 1277–1280.
- Tarling, D. H. and Hrouda, F., 1993. *The magnetic anisotropy of rocks*. Chapman and Hall, London.
- Van Dongen, P. G., Van der Voo, R., Ravan, Th. 1967. Paleomagnetism and the Alpine tectonics of Eurasia III. Paleomagnetic research in the Central Lebanon Mountains and the Tartous area of Syria: *Tectonophysics*, 4, 35–53.